EUROPEAN ORGANIZATION FOR NUCLEAR RESEARCH

CERN-EP/89-83
10 July 1989

FULL ANGULAR DISTRIBUTION OF THE ANALYSING POWER IN $\bar{p}p$ ELASTIC SCATTERING AT 697 MeV/c

R. Bertini[1], M. Costa[2] and F. Perrot[1]
CERN, Geneva, Switzerland

H. Catz, A. Chaumeaux, J.Cl. Faivre and E. Vercellin[2]
DPhN/ME CEN-Saclay, Gif-sur-Yvette, France

J. Arvieux and J. Yonnet
Laboratoire National Saturne, CEN-Saclay, Gif-sur-Yvette, France

B. van den Brandt, J.A. Konter, D.R. Gill[3], S. Mango and G.D. Wait[3]
Paul Scherrer Institute, Würenlingen and Villigen, Switzerland

E. Boschitz, W. Gyles, W. List, C. Otterman, R. Tacik and M. Wessler
Univ. Karlsruhe and Kernforschungzentrum Karlsruhe, Fed. Rep. Germany

E. Descroix, J.Y. Grossiord and A. Guichard
IPN Univ. Claude Bernard Lyon 1 and CNRS-IN2P3, Villeurbanne, France

ABSTRACT

Full angular distributions of the differential cross-section $d\sigma/d\Omega$ and of the analysing power A_y in $\bar{p}p$ elastic scattering have been measured at 697 MeV/c. The results of A_y are compared with the predictions of various theoretical models.

(Submitted to Physics Letters B)

Present addresses:
1) DPhN/ME, CEN-Saclay, Gif-sur-Yvette, France.
2) Istituto Nazionale di Fisica Nucleare, Turin, Italy.
3) TRIUMF, Vancouver BC, Canada.

The theoretical approach to $\bar{N}N$ scattering is based mainly on potential models. The first ingredient of this approach is a form of theoretical NN potential, based on meson exchange, which is G-parity transformed to an $\bar{N}N$ potential. This G-parity transformation reverses the signs of the potential contributions of the odd G-parity meson exchanges. The second ingredient in $\bar{N}N$ models is some kind of annihilation mechanism. The annihilation cross-section is large ($\sigma_{ann}/\sigma_{el} \geq 2$) and is responsible for the large imaginary part of the potential. There are several different approaches to this annihilation: one may apply a suitable boundary condition [1], or use an optical potential [2–5], or do a coupled-channel calculation [6], or assume that one $\bar{q}q$ pair annihilating into gluons is the dominant channel for the $\bar{N}N$ annihilation [7]. All these approaches fit the existing data on the spin-averaged cross-sections reasonably well. For the spin-dependent observables, the situation is completely different: the predictions depend consistently on the theoretical inputs. Therefore the measurement of spin observables in the $\bar{p}N$ elastic scattering will provide useful constraints to define the proper set of parameters of the $\bar{N}N$ potentials—provided the data are obtained over the full angular range—because the different theoretical predictions differ significantly in different angular domains. This was the main motivation of the experiment PS198 performed with the antiproton beam of the Low-Energy Antiproton Ring (LEAR) at CERN.

We report here the first measurement of the full angular distribution of the differential cross-section $d\sigma/d\Omega$ and of the analysing power A_y in the $\bar{p}p$ elastic scattering at 697 MeV/c. Data on $d\sigma/d\Omega$ near this energy have already been published [8, 9]. With regard to A_y, a few points with large error bars have been measured in a double-scattering experiment [10], and recently, data have been produced in a more restricted angular domain at 679 and 783 MeV/c [11].

The experimental set-up is illustrated in fig. 1. Monitoring of the beam was done by the counter (1). This counter consisted of a thin scintillator (F), 0.3 mm thick, and of an antihalo scintillator (FH), 0.5 mm thick, with a circular hole 12 mm in diameter. The scintillators F and FH were individually viewed by two phototubes in coincidence; FH was put in anticoincidence with F to give the signal F0. When the beam was focused on the polarized target (2), typical counting rates of FH were less than 2% of F. Additional relative monitoring was provided by counter M (3), which consisted of two slabs of scintillator placed in view of the target at 0° and out of the scattering plane and of the acceptance of the spectrometer. The polarized target consisted of a slab of pentanol ($C_5H_{12}O$), 5 mm thick, 18 mm high, and 18 mm wide, doped with ethyl hydroxybuteric acid (EHBA). The 2.5 T magnetic field, which was needed to polarize the protons, was produced by a superconducting split-coil magnet supplying a vertical field. The proton polarization was determined by comparing the dynamic polarization signal with the natural polarization signal at thermal equilibrium. Polarization values of 0.68 to 0.85 were obtained. In order to decrease the influence of the magnetic field on the trajectories of the incoming and outgoing particles, we lowered the target field to 0.7 T, operating it in frozen-spin mode. The proton relaxation time was about 150 h.

The scattered particles were detected and momentum-analysed with the magnetic spectrometer SPESII [12]. In order to cover the full angular domain in the c.m. system, we detected the $\bar{p}$'s for the forward c.m. angles and the recoil p's for the backward ones, rotating SPES II and/or reversing its magnetic field to get the appropriate c.m. angular set. The detection system of the spectrometer consisted (fig. 1) of four multiwire proportional chambers (MWPC), CH0, ..., CH3, all of them with X and Y planes, and of a scintillator counter S. The acceptance of the spectrometer was defined by CH0. The angle and the momentum of the scattered particles were measured with CH1, CH2, and CH3. These three chambers and counter S were put on a movable carriage, the position of which was changed at each scattering angle so that the focal plane always crossed CH2, independent of its kinematical recoil. The trigger was F0*S, and the precise time-of-flight measurement made with these two counters discriminated the $\bar{p}$'s and the p's, respectively, from the other products (mainly pions)

of the interaction of the $\bar{p}$ beam with the target. A complete retracking was performed in two ways, with the X, Y, θ, and ϕ coordinates at the focal plane and the transfer matrix of SPESII: i) Using chamber CH0 at the entrance of SPESII (40 cm downstream from the polarized target), the computed X and Y coordinates of CH0 were compared with the measured ones. The differences between these two sets of coordinates enabled the point of origin of the track to be determined. In this way, spurious tracks coming from the antiproton counter F, or from the windows or the thermal screens of the polarized target, could be rejected. ii) The complete reaction kinematics was reconstructed at the position of the target, yielding the missing mass. In this way we could select the $\bar{p}p$ elastic channel from the contributions of nuclei other than the target protons. Around $\theta_{lab} \approx 45°$, where the energy of the detected particle was minimal, the angular and energy stragglings considerably deteriorated the resolution for the missing mass. In order to investigate possible contamination from quasi-elastic scattering or other reactions on the nuclear content of the target, we added a recoil counter R [(9) in fig. 1], which was placed at an angle of about 90° with respect to the direction of the scattered particle and rotated with SPESII. This counter consisted of a scintillator slab and a MWPC, with X and Y planes. Its acceptance corresponded to the full aperture of SPESII and was efficient for the detection of the recoil particle, p or $\bar{p}$, in the angular domain $70° \leq \theta_{cm} \leq 110°$. Track reconstruction and coplanarity selection showed that quasi-elastic contamination was negligible even in that angular domain. We checked our apparatus during a preliminary run with a proton beam, measuring $d\sigma/d\Omega$ in pp elastic scattering. Our results were consistent with the phase-shift analysis of ref. [13].

In $\bar{p}p$ elastic scattering, the angular distribution of the spin-averaged cross-section $d\sigma/d\Omega$ has been fitted with the Legendre polynomial expansion:

$$d\sigma/d\Omega(\theta) = \sum_{\ell} a_\ell P_\ell(\cos\theta) \ .$$

The data together with the best-fit curve are shown in fig. 2. Coulomb interference does not affect this analysis since only angles $\theta_{cm} > 20°$ have been taken into account. The best-fit coefficients a_ℓ are presented in table 1 and compared with those given in refs. [8], [9] and [14]. It appears that the agreement is particularly good with the coefficients from ref. [9]. The angular distribution of A_y has been fitted with the associated Legendre polynomial expansion:

$$(d\sigma/d\Omega)A_y = \sum_{\ell} b_\ell P_\ell^1(\cos\theta) \ .$$

The data together with the best-fit curve are shown in fig. 3a. The best-fit coefficients b_ℓ are also presented in table 1.

The angular distribution of A_y at 700 MeV/c has been calculated in ref. [15], using the Bryan-Scott one-boson exchange potential and the black-sphere annihilation model with cut-off parameters $\Lambda = 980$ MeV and 1040 MeV. The results are shown in fig. 3a.

In fig. 3b, the A_y data have also been compared with the theoretical predictions given by the Dover-Richard I (DRI) model [16], the PARIS model [5], the Bryan and Phillips potential [2], and the Nijmegen group [6]. To keep the figure clear, we have not shown other predictions such as those based on DRII [16] or the ones given in ref. [17], which differ more significantly from our data. This selection has been somewhat arbitrary, as even the calculations that have been selected for fig. 3b reproduce, at most, only the general trend of the data. A reasonable agreement with our data is provided by the calculations shown in fig. 3a where, instead of an optical potential, a much simpler black-sphere model has been chosen to describe the annihilation. However, even this approach fails to reproduce the dip shown by the data around $\cos\theta_{cm} = -0.2$. This comparison between various

theoretical calculations and our measurements leads us to the conclusion that none of them fits our data really well. The disagreement is more or less pronounced in different angular regions, reflecting the different weight given to the various helicity amplitudes in the models, which have therefore to be studied again in order to satisfy the new constraints provided by our data.

We gratefully acknowledge the assistance of CERN, and in particular of the LEAR operating crew. We are very much indebted to the technical groups from DPhN/ME and LNS, Saclay, for their help in realizing the experiment.

REFERENCES

[1] A. Delville et al., Am. J. Phys. **46** (1978) 907.
O.D. Dalkarov and F. Myhrer, Nuovo Cimento **40A** (1977) 152.
[2] R.A. Bryan and R.J.N. Phillips, Nucl. Phys. **B5** (1968) 201.
[3] W.W. Buck, C.B. Dover and J.M. Richard, Ann. Phys. **121** (1979) 47.
C.B. Dover and J.M. Richard, Ann. Phys. **121** (1979) 70.
C.B. Dover and J.M. Richard, Phys. Rev. **C21** (1980) 1466.
[4] T. Ueda, Prog. Theor. Phys. **62** (1979) 1670.
[5] J. Cote et al., Phys. Rev. Lett. **48** (1982) 1319.
[6] P.H. Timmers et al., Phys. Rev. **D29** (1984) 1928.
[7] R. Tegen et al., Phys. Lett. **182B** (1986) 6.
[8] E. Eisenhandler et al., Nucl. Phys. **B113** (1976) 1.
[9] T. Kageyama et al., Phys. Rev. **D35** (1987) 2655.
[10] M. Kimura et al., Nuovo Cimento **A71** (1982) 438.
[11] R.A. Kunne et al., Phys. Lett. **B206** (1988) 557.
[12] H. Catz, thesis, Note CEA-N-**2251** (1981).
[13] F. Lehar et al., J. Phys. (France) **48** (1987) 1273.
[14] R.A. Kunne et al., preprint CERN-EP/88-171 (1988), to appear in Nuclear Physics B.
[15] T. Mizutani, F. Myhrer and R. Tegen, Phys. Rev. **D32** (1985) 1663.
[16] C.B. Dover and J.M. Richard, Phys. Rev. **C25** (1982) 1952.
[17] J.C.H. van Doremalen, Yu.A. Simonov and M. van der Velde, Nucl. Phys. **A340** (1980) 317.

Table 1

Legendre fit coefficients

a_ℓ	This exp.	Kageyama et al. [9]	Eisenhandler et al. [8]	Kunne et al. [14]	b_ℓ	This exp.
a_0	3.59 ± 0.02	3.57 ± 0.01	4.22 ± 0.07			
a_1/a_0	2.22 ± 0.02	2.22 ± 0.01	2.30 ± 0.05	2.57 ± 0.08	b_1/a_0	0.174 ± 0.004
a_2/a_0	2.32 ± 0.02	2.28 ± 0.01	2.51 ± 0.07	2.58 ± 0.10	b_2/a_0	0.171 ± 0.005
a_3/a_0	1.46 ± 0.02	1.42 ± 0.01	1.73 ± 0.07	2.07 ± 0.10	b_3/a_0	0.136 ± 0.004
a_4/a_0	0.53 ± 0.02	0.55 ± 0.01	0.81 ± 0.05	1.10 ± 0.06	b_4/a_0	0.062 ± 0.004
a_5/a_0	0.11 ± 0.01	0.11 ± 0.01	0.26 ± 0.05	0.45 ± 0.02	b_5/a_0	0.020 ± 0.002
a_6/a_0		0.003 ± 0.01			b_6/a_0	0.006 ± 0.001

Figure captions

Fig. 1 Experimental set-up (not to scale): 1) antiproton counters F and FH; 2) polarized target; 3) monitor counter M, out of the plane of the figure; 4) MWPC C0; 5) spectrometer SPESII; 6) MWPCs CH1, CH2, and CH3; 7) scintillator S; 8) focal plane; 9) recoil counter R.

Fig. 2 Angular distribution of $d\sigma/d\Omega$. The curve represents the best fit with Legendre polynomials.

Fig. 3 The data of the analysing power A_y. They are compared with the theoretical predictions of:
a) ref. [15] with the cut-off parameters Λ = 980 MeV and 1040 MeV; the solid line represents the best fit with Legendre polynomials;
b) Dover–Richard [16] (solid line), Paris [5] (dash-dotted curve), Nijmegen [6] (dashed curve), and Bryan–Phillips [2] (dotted curve).

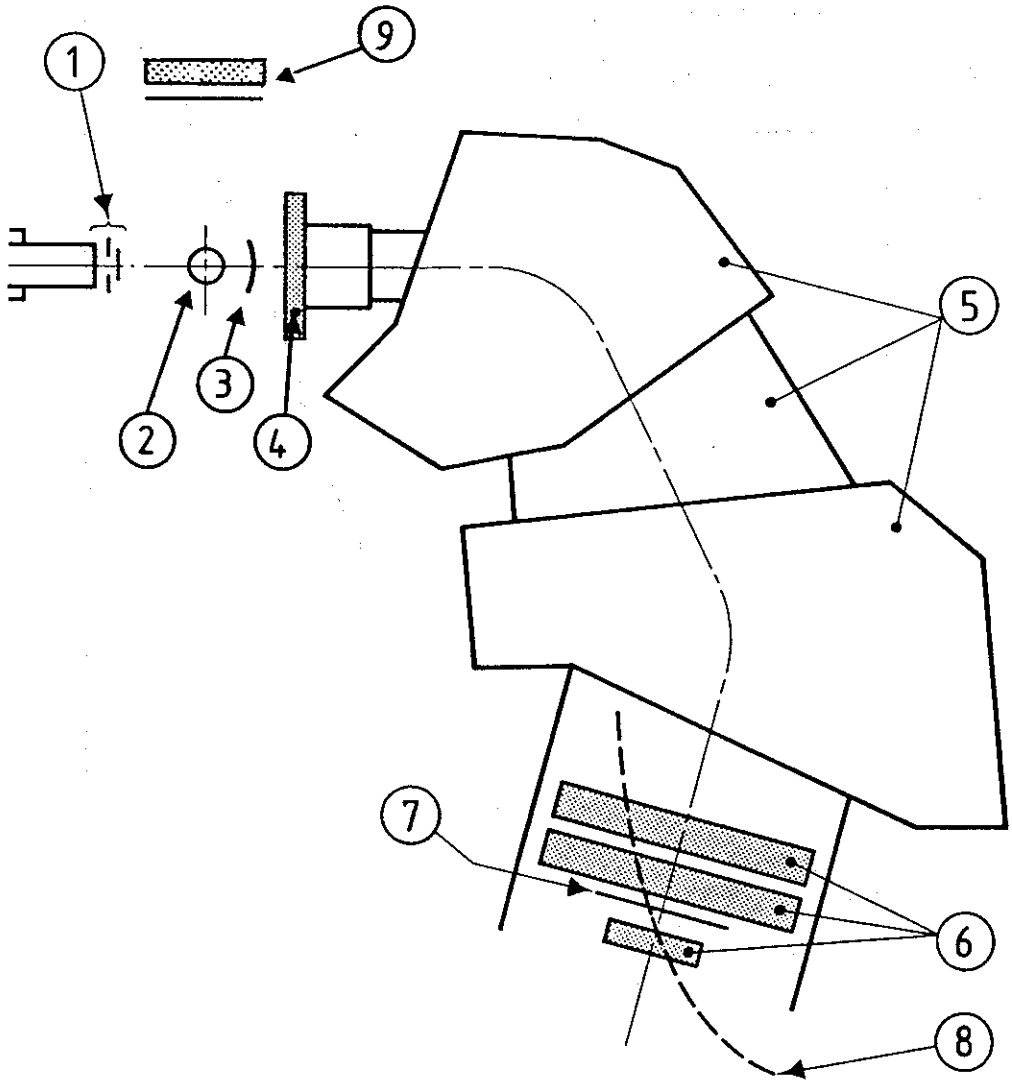

Fig. 1

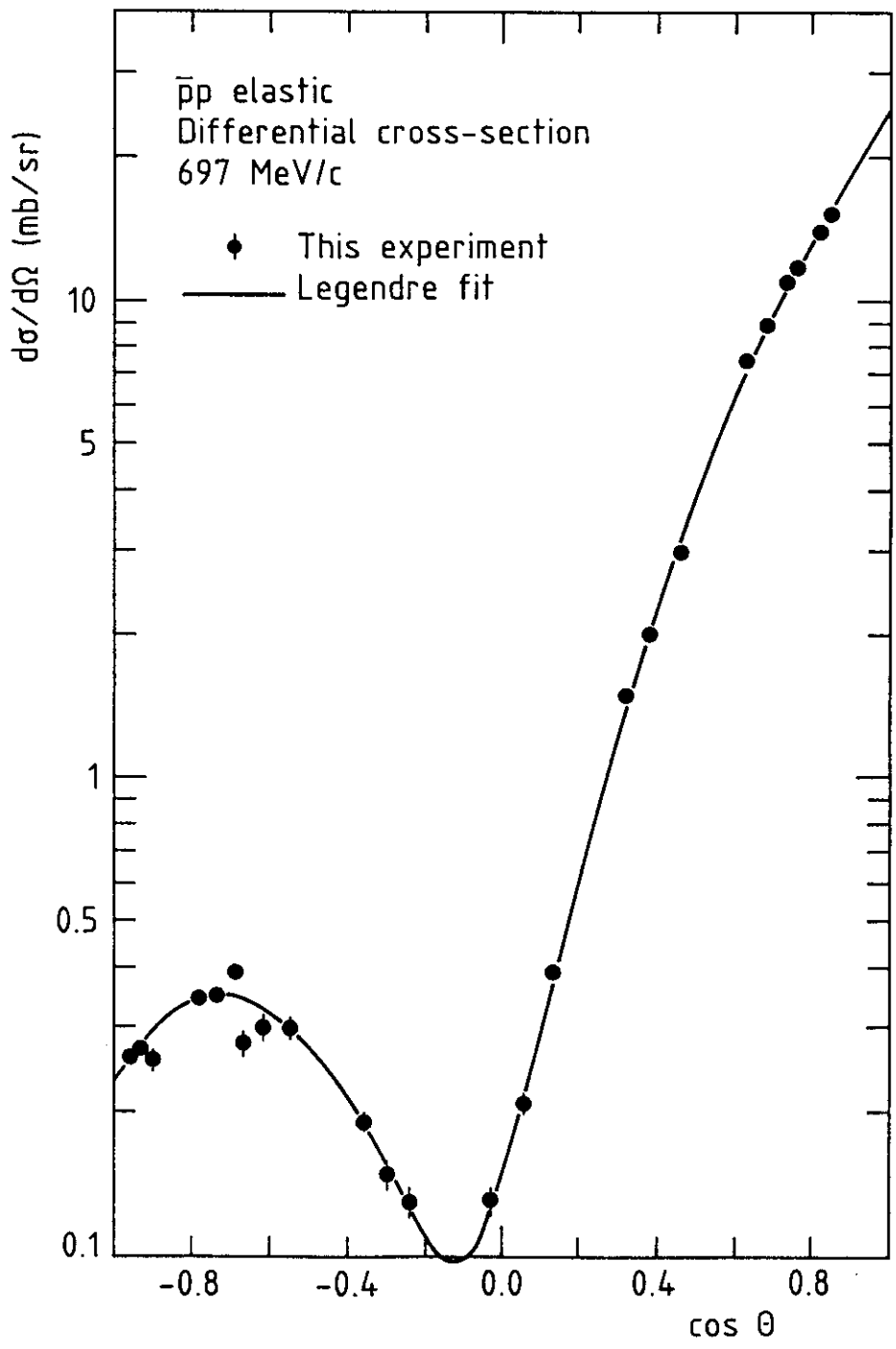
p̄p elastic
Differential cross-section
697 MeV/c
This experiment
Legendre fit
dσ/dΩ (mb/sr)
10
5
1
0.5
0.1
-0.8
-0.4
0.0
0.4
0.8
cos Θ

Fig. 2

a)

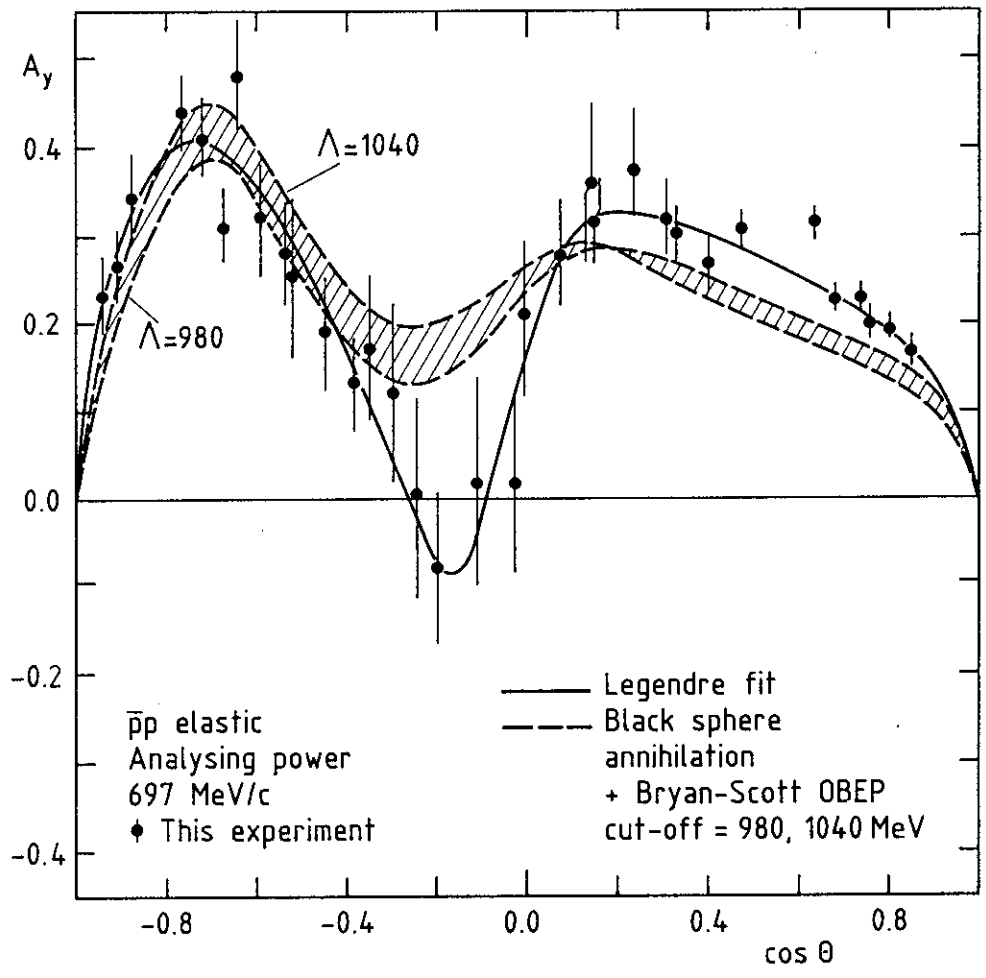
A_y
0.4
0.2
0.0
-0.2
-0.4
Λ=1040
Λ=980
p̄p elastic
Analysing power
697 MeV/c
♦ This experiment
Legendre fit
Black sphere
annihilation
+ Bryan-Scott OBEP
cut-off = 980, 1040 MeV
-0.8
-0.4
0.0
0.4
0.8
cos θ

b)

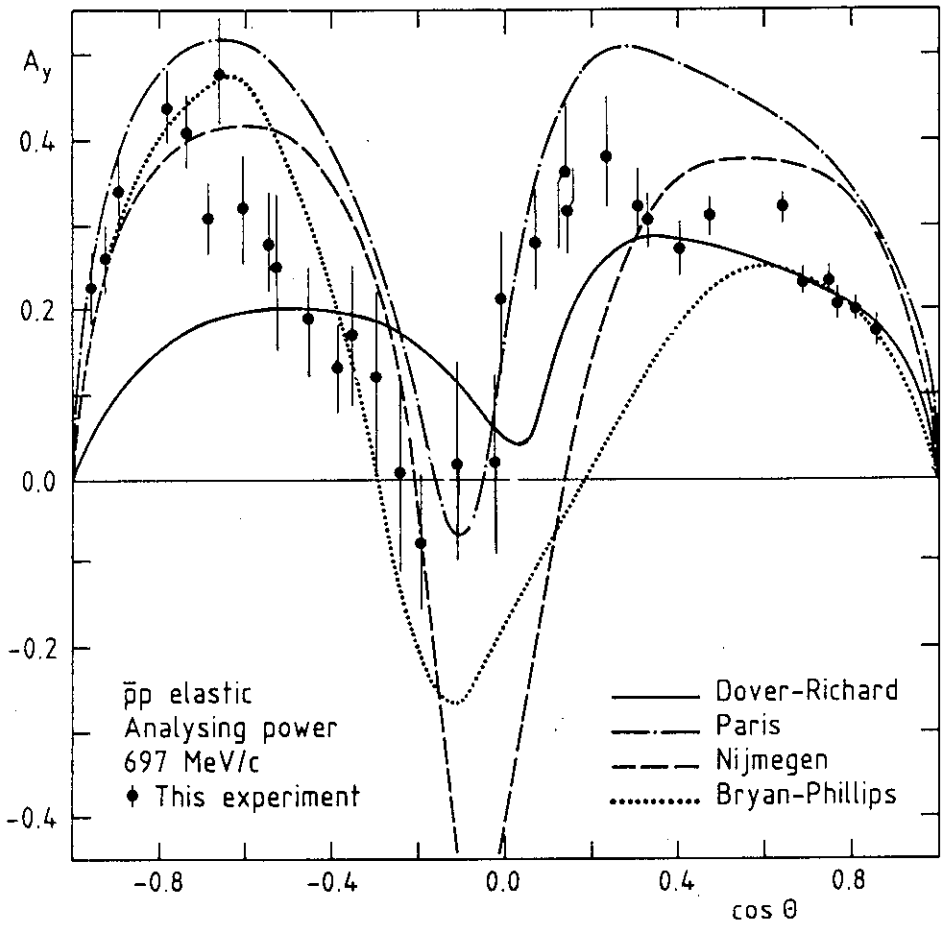
A_y
0.4
0.2
0.0
-0.2
-0.4
p̄p elastic
Analysing power
697 MeV/c
♦ This experiment
Dover-Richard
Paris
Nijmegen
Bryan-Phillips
-0.8
-0.4
0.0
0.4
0.8
cos θ

Fig. 3